3

Field Observation in the North Basin

S. Endoh, Y. Okumura and I. Okamoto

Introduction

As mentioned in the previous section, a great number of observations have been carried out in the last 30 years to clarify the structure of the currents associated with the gyres in the North Basin of Lake Biwa. In this section, some results from current measurements of the gyres are described. The two main observational techniques have been buoy-tracking and continuous current metering. These methods have steadily improved over the years and it is now possible to obtain accurate and dense data on the current field. Various materials have been used for drogues such as drift bottles, cross boards, drift cylinders, and window-shades. Buoy-tracking has been carried out using distance meters, magnetic compass, sextants, radio transceivers, radar, balloons, aircraft and satellites. By comparison, fixed current meters have a short history (about ten years) in Lake Biwa, but a great deal of information has already been accumulated using improved instrumentation and mooring methods.

Drifter Tracking

In August of 1979, five buoys with window-shade drogues at a depth of 2 m were released in the central area of the North Basin around observation stations A-D, M, O, S. (Figure 3.1) and tracked by boat for several hours. A sextant was used to determine the positions of the buoys to an accuracy of about 100 m. The wind was rather weak

Physical Processes in a Large Lake: Lake Biwa, Japan
Coastal and Estuarine Studies, Volume 48, Pages 15–29

throughout the observation period. Figures 3.2a and 3.2b show the trajectories of thesebuoys on August 24 and 25, 1979 which indicate the existence of a large cyclonic gyre, the First Gyre. Current velocities ranged from 0.1 to 0.2 m s^{-1} throughout the three day observation period. On August 26, eight buoys were tracked using two boats. Once again a stable cyclonic gyre was observed (Figure 3.2c).

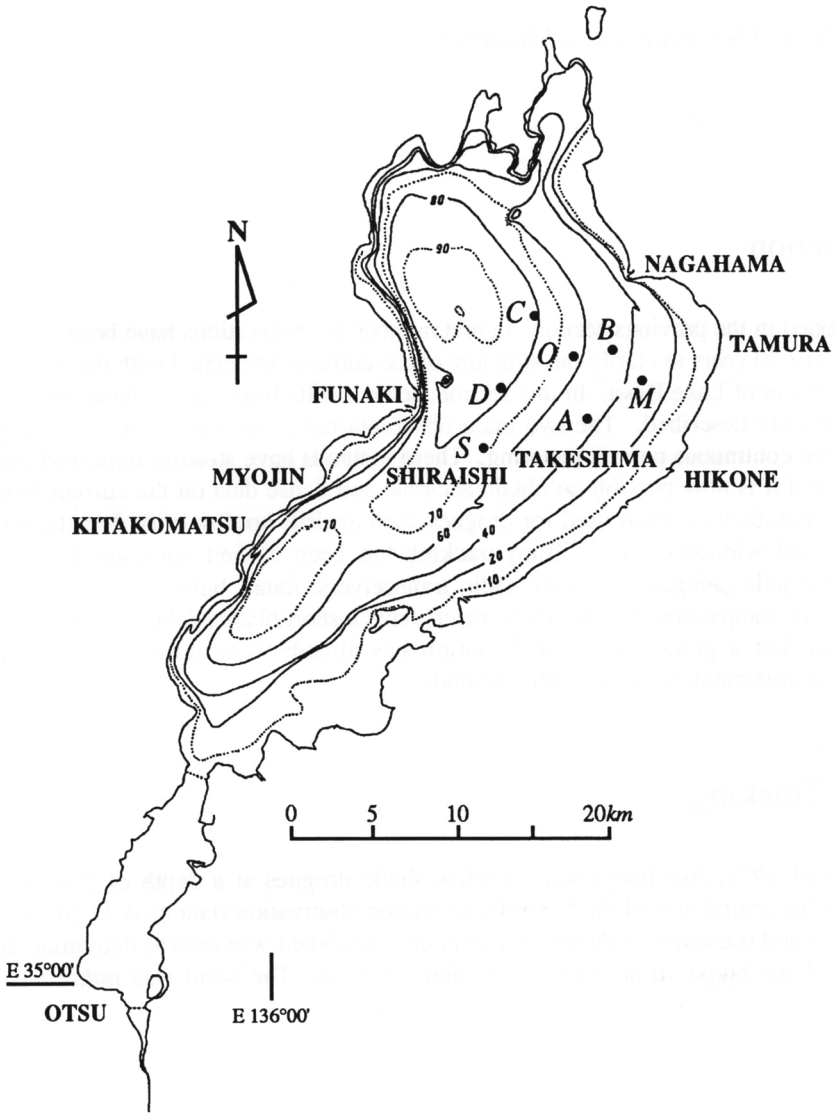

Figure 3.1. Map of Lake Biwa showing some observation stations. Depth contours are in meters.

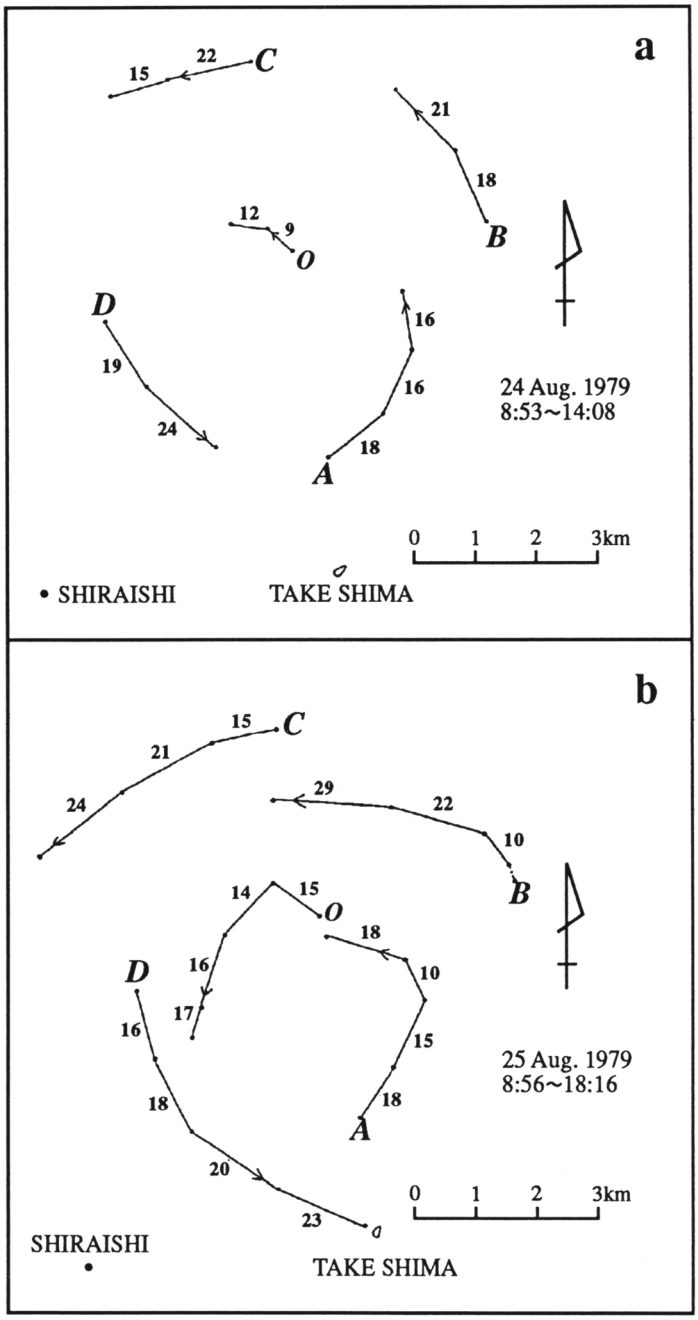

Figure 3.2. Trajectories of the buoys tracked by a boat with a sextant on August 24-26, 1979. The numerals beside the trajectories represent the current speed in cm s^{-1}

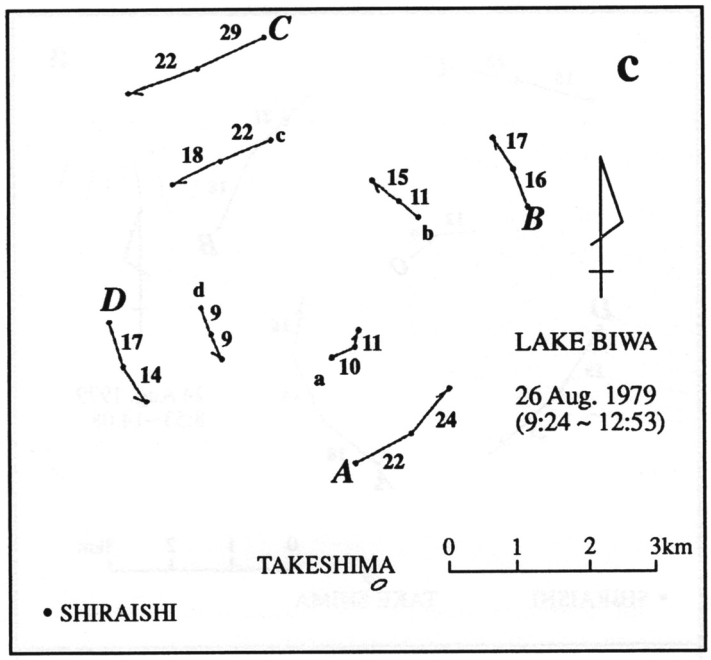

Figure 3.2 (Continued)

During the current observations, the three dimensional water temperature distribution was measured with a bathythermograph from another boat. Figure 3.3a shows vertical sections of water temperature along a cross section through Stations D, O and B, averaged over the period from August 24 to 25. A domed isotherm structure was observed within the gyre leading to a cold central core, corresponding to a geostrophic balance. The geostrophic current distribution calculated from this temperature distribution is shown in Figure 3.3b. The reference level was assumed to be located at the 30 dbar layer. Good agreement with the measurements shown in Figure 3.2 is apparent.

Figure 3.4 shows the dynamic height topography referenced to the 30 dbar layer and calculated using the water temperature distribution. The trajectories of the drifters are included to show that the drifter paths closely followed the dynamic height contours.

The horizontal divergence was estimated by calculating the time-change of the triangular area separated by three drifters. The result shows that the water in this gyre had a tendency to converge at a rate of 10^{-5} s^{-1} similar to that estimated with the diagnostic model (Endoh, 1978). Figure 3.5 shows the vertical circulations calculated with a diagnostic model using the water temperature distribution shown in Figure 3.3a; two-cell circulations can be seen sinking near the gyre centre and spreading at the thermocline. Endoh (1986) pointed out that the resulting vertical circulation represented a decaying gyre. In general the vertical circulation will play an important role in metabolic and sedimentation processes and thus the distribution of suspended materials.

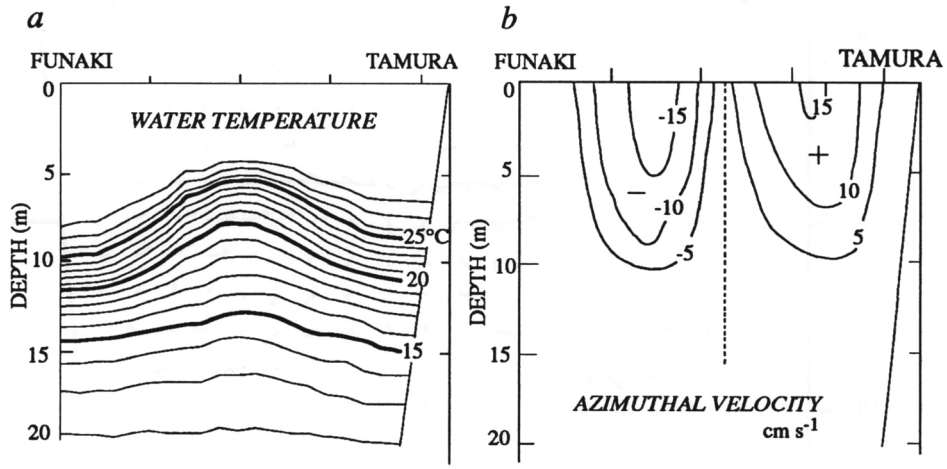

Figure 3.3. A vertical section of (a) water temperature averaged over August 24 and 25, 1979; (b) geostrophic current velocity calculated using water temperature with the reference level of 30 dbar.

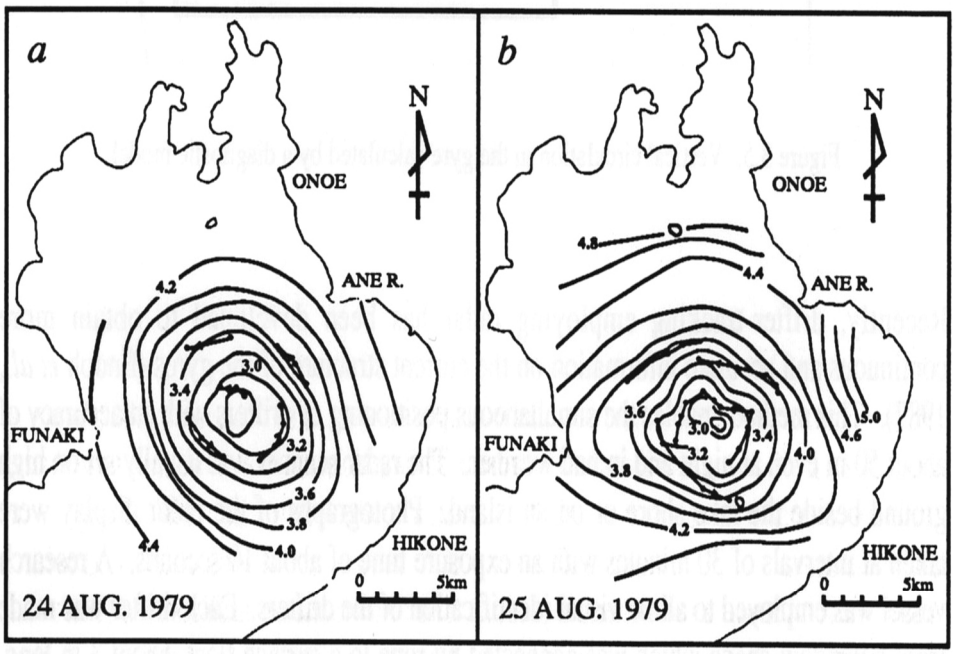

Figure 3.4. Dynamic height topography at the surface referenced to 30 dbar surface on (a) August 24 and (b) August 25, 1979. The trajectories of buoys are also shown.

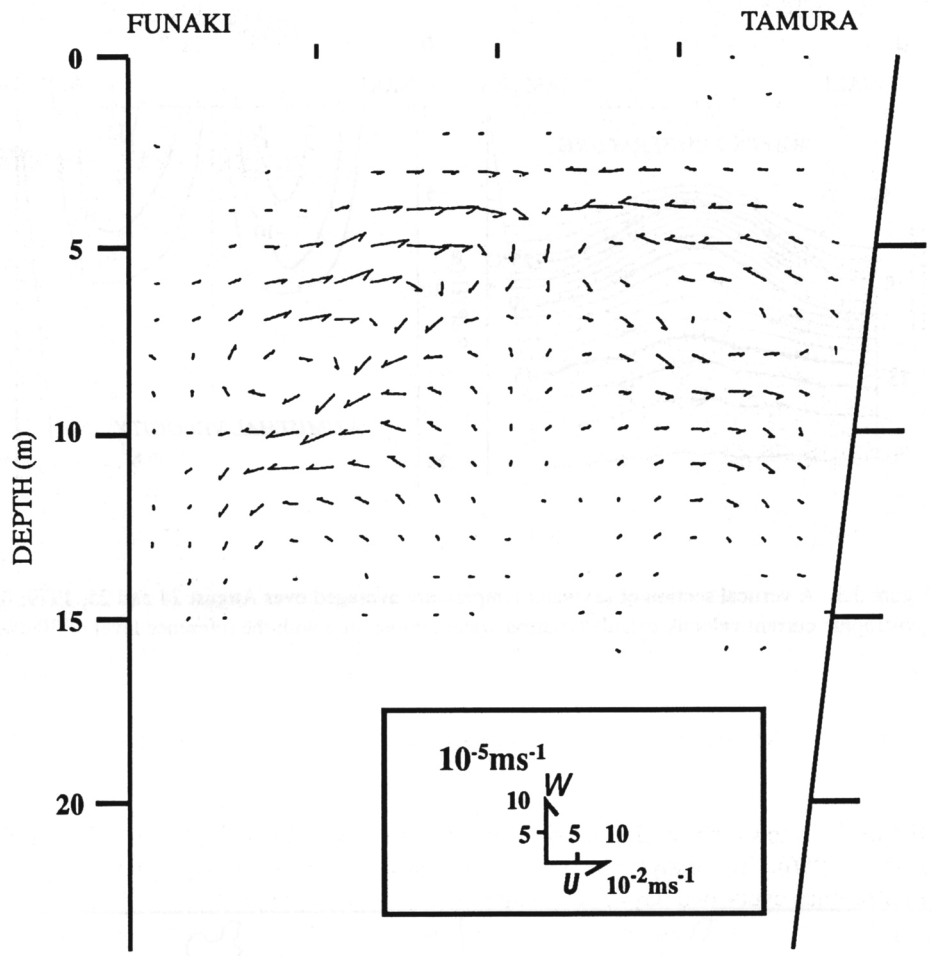

Figure 3.5. Vertical circulation in the gyre calculated by a diagnostic model.

Recently, drifter-tracking employing radar has been developed to obtain more continuous and accurate information on the current structure of the gyres (Endoh *et al.*, 1987). This method enables the simultaneous positioning of drifters with an accuracy of about 50 m even at night and in bad weather. The radar scanner was usually set on high ground beside the lake shore or on an island. Photographs of the radar display were taken at intervals of 30 minutes with an exposure time of about 10 seconds. A research vessel was employed to allow visual identification of the drifters. Each drifter was made from a window-shade which was connected by rope to a surface float, about 3 m long, with a corner reflector on the top. An example of a radar display is shown in Figure 3.6, taken at Takeshima Island in 1983. The several white points in the lake (the dark area) represent the echoes from the drifters.

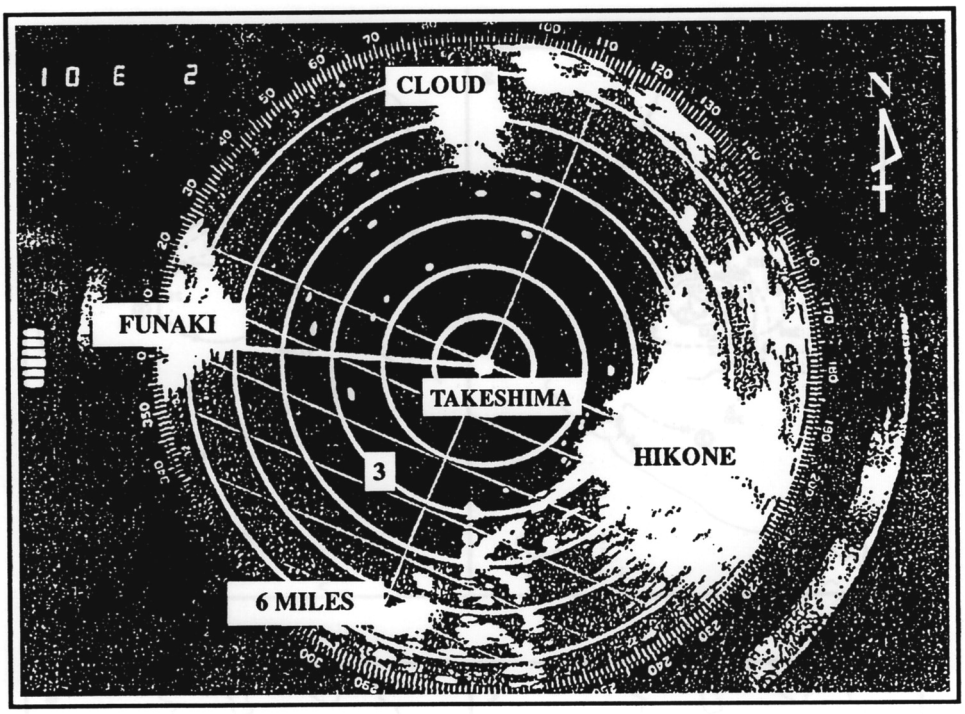

Figure 3.6. A picture of a radar display taken at Takeshima at 300 UT on September 2, 1983.

Figure 3.7 shows the results of drifter-trackings using radar in September, 1983 (after Endoh, 1986). The buoys which were drogued at a depth of 5 m (Figures 3.7a, 3.7b) rotated once every two days in a counter-clockwise direction, but some of them moved southward away from the gyre; the latter movements being caused by internal Kelvin waves which were also detected by the current meters (Endoh, 1986). Figure 3.7c shows four trajectories of drifters drogues at a depth of 10 m; these had tracks very close to a true circle due to the decreased effect of internal waves just above the thermocline.

Horizontal convergence was observed with every buoy at this depth, each moving towards the gyre centre with a radial velocity of about 5×10^{-3} m s^{-1}. Figure 3.7d shows the movements of deeper buoys (20 m and 30 m deep); here a very slow current speed was observed in the same direction as the surface layer. However, these deep drogues were influenced greatly by the overlying stronger currents. Once corrected for heavy drift (Endoh *et al.*, 1987), these drogues revealed that below the thermocline the water was almost stationary.

The Second Gyre (clockwise) has been frequently observed towards the south of the First Gyre. Because this gyre is anti-cyclonic (in a direction opposite to the earth's rotation), it is sometimes difficult to detect the structure of this gyre by water temperature distributions because of differences in the gyre dynamics. The pressure

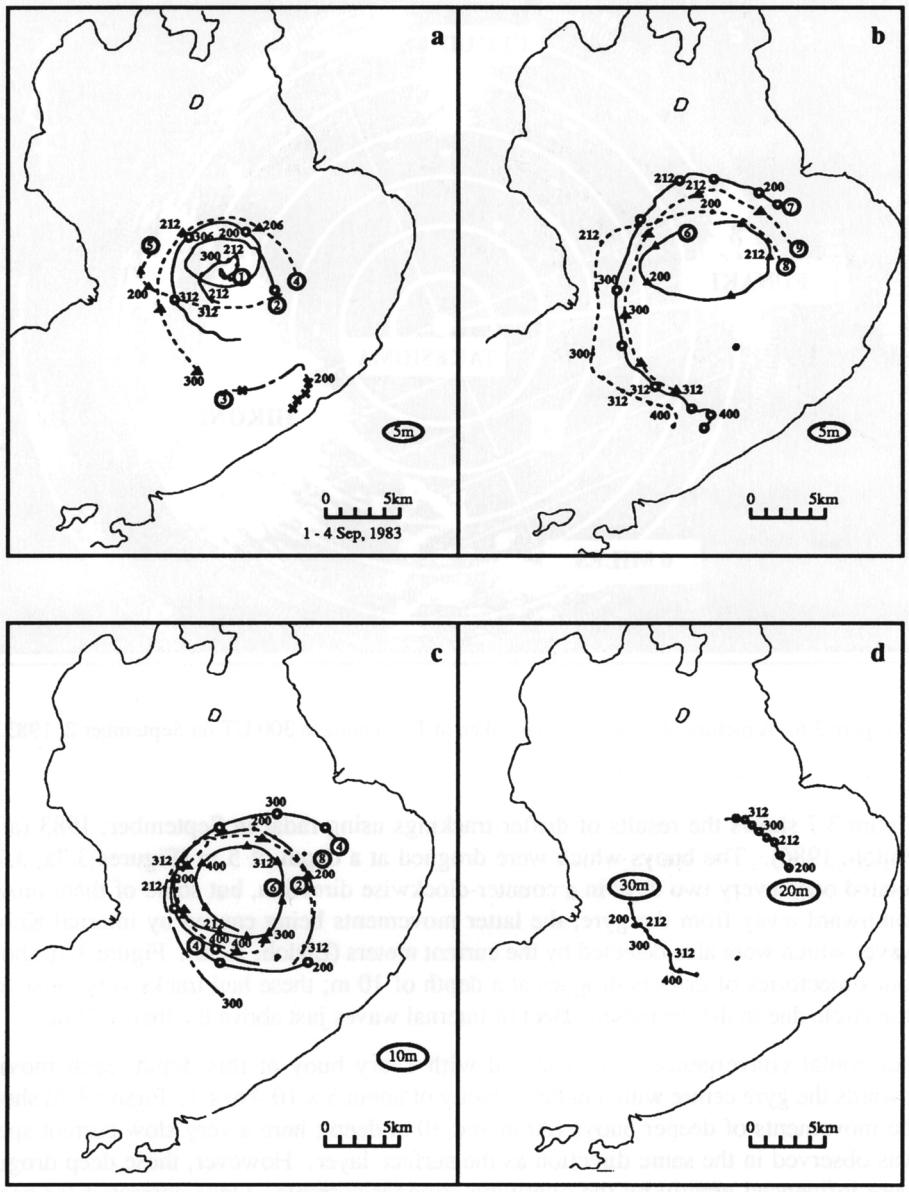

Figure 3.7 Trajectories of drifters at several depths on September 1-4, 1983. (a) and (b) at 5 m depth; (c) at 10 m depth; (d) at 20 m and 30 m depth. Numerals beside the trajectories show the day and hour e.g. 212 means 1200UT on September 2 (after Endoh, 1986; Endoh *et al.*, 1987).

gradient force (produced by temperature differences) is usually stronger in a cyclonic gyre because the Coriolis force and centrifugal forces are added. In an anti-cyclonic gyre the forces counteract each other resulting in a weaker feature.

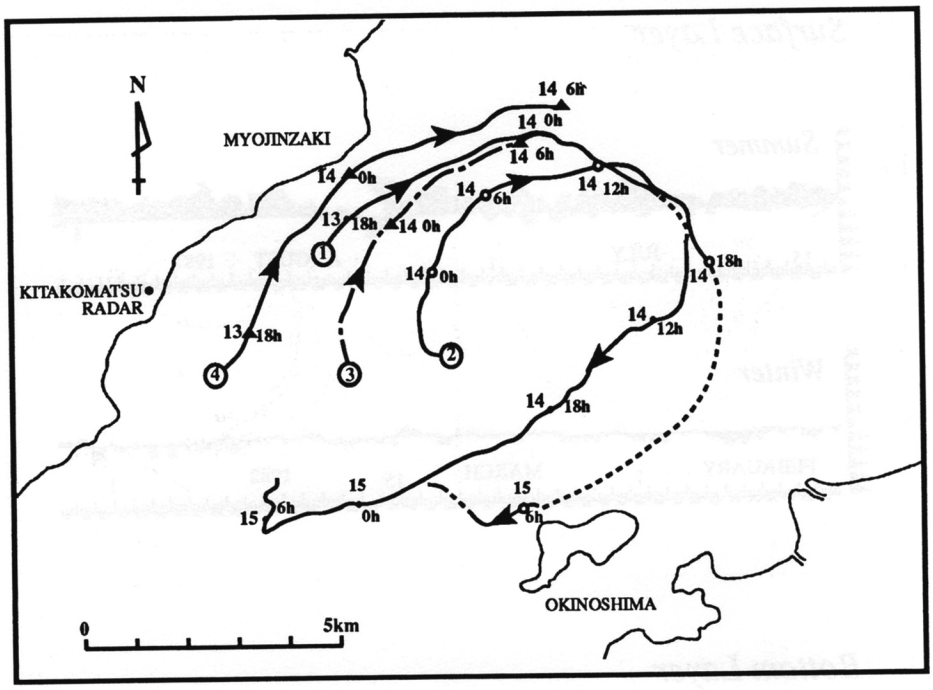

Figure 3.8. Trajectories of four drifters at a depth of 5 m showing the clockwise Second Gyre, September 13-15, 1986 (after Endoh *et al.*, 1987).

The best way to clarify the current structure of the Second Gyre is by direct current measurements. In September of 1986, several drifters were released and tracked by radar at Kitakomatsu. The method was almost the same as that described above. Figure 3.8 shows the trajectories of some of these drifters between September 13 and 15, 1986. All the drifters moved clockwise at a speed of between 0.1 and 0.2 m s^{-1}. The shape of this gyre was more elliptical, quite different from the circle-shaped First Gyre. The trajectories and current meters indicated the occasional development of a coastal jet, near Myojinzaki on the the western shore, with a maximum current speed of 0.4 m s^{-1}.

Measurement by Current Meters

Since 1981, a number of current measurements have been carried out using automated current meters including the RCM-4 (Aanderaa) and DCM-3 (Osaka Electro-Communication University) (Okumura and Endoh, 1985: Endoh and Okumura, 1989). These current meters allow the continuous measurement of current speed, direction, and water temperature for about one month.

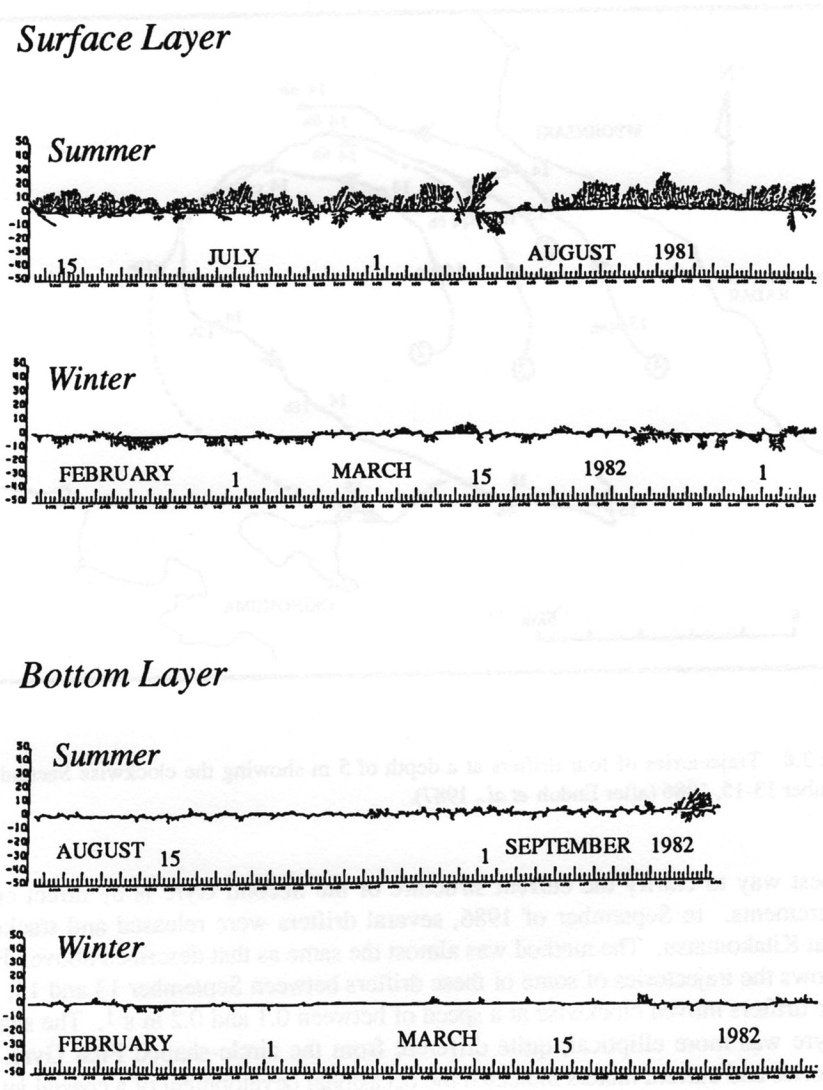

Figure 3.9 Diagrams of time series of current vectors. Upper: the surface layer in summer and winter; lower: the bottom layer in summer and winter (after Okumura and Endoh, 1985).

The horizontal and vertical structure and time-variation of the current in Lake Biwa is somewhat unusual. In particular, the current field in winter and in the deep layer is poorly understood. Figure 3.9 shows the results of current measurements at the surface and at depth during summer and winter around Station M (Figure 3.1), about 5 km northwest of Hikone. Current vectors are shown, for each 10 minutes, for a period of about a month. In this figure, the strong and stable current in the surface layer in the summer is evident, as well as the relatively weak current in the winter. This is due to the existence

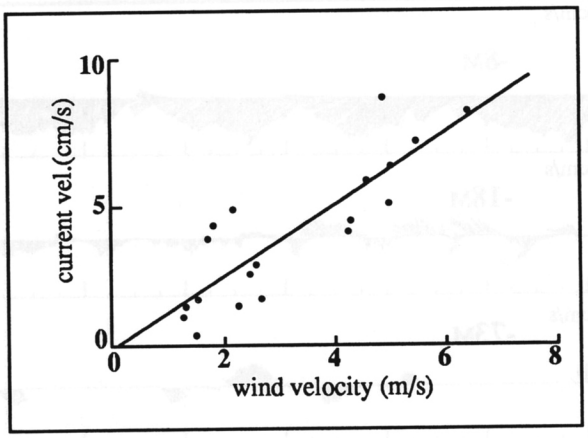

Figure 3.10. Scatter diagram of daily averaged current speed and wind speed. Correlation coefficient is 0.85 (after Okumura and Endoh, 1985).

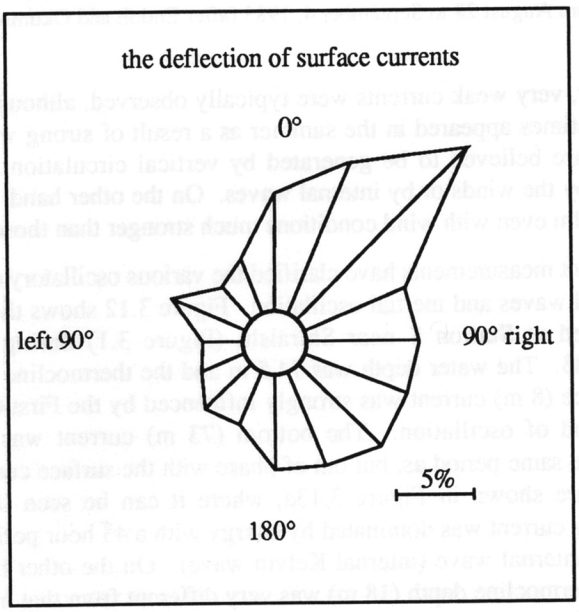

Figure 3.11. Frequency diagram of deflection of the current direction from the wind direction (after Okumura and Endoh, 1985).

of the gyre current in summer. In winter, no well defined gyre exists and the current field is therefore controlled by the wind. The correlation between the current and the wind velocity was high; the observed current was about 1/80 of the wind velocity (Figure 3.10). The surface current direction in winter was slightly deflected to the right of the wind direction by the formation of a weak Ekman drift (Figure 3.11).

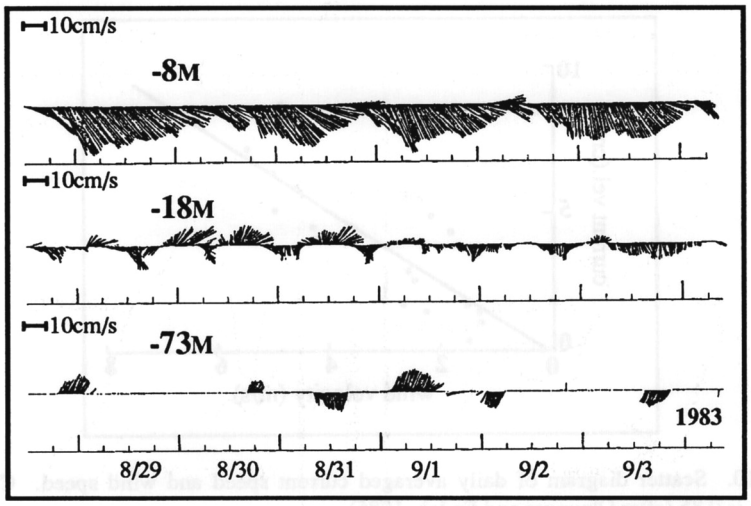

Figure 3.12. Stick diagrams of current in three layers (surface, thermocline and bottom) taken near Okino-shiraishi from August 28 to September 4, 1983 (after Endoh and Okumura, 1989).

In the deep layer, very weak currents were typically observed, although high velocities (0.2 m s^{-1}) sometimes appeared in the summer as a result of strong winds. Such deep strong currents are believed to be generated by vertical circulation or compensating currents caused by the winds or by internal waves. On the other hand, the deep layer in winter is quite calm even with wind conditions much stronger than those during summer.

Continuous current measurements have clarified the various oscillatory current structures including internal waves and inertial oscillation. Figure 3.12 shows the vertical current variation obtained at Station S near Shiraishi (Figure 3.1) during August 28 and September 4, 1983. The water depth was 74.5 m and the thermocline depth was about 15 m. The surface (8 m) current was strongly influenced by the First Gyre motion and had a long period of oscillation. The bottom (73 m) current was very weak and oscillated with the same period as, but out of phase with the surface current. The rotary current spectra are shown in Figure 3.13a, where it can be seen that the counter-clockwise rotating current was dominated by energy with a 43 hour period; indicative of the fundamental internal wave (internal Kelvin wave). On the other hand, the current variation at the thermocline depth (18 m) was very different from that in the surface and bottom layers. The period was shorter and the current direction varied in a clockwise fashion with time. The rotary spectra shown in Figure 3.13b indicate a steep spectral peak at 21 hour; the inertia period in the Lake Biwa basin. As shown in Figure 3.13a, there were no spectral peaks at this period in the surface and bottom layers. Following both observations it can be noted that the thermocline depth corresponds to the "level of no motion" for the long-period internal wave as well as marking the bottom of the gyre current. If a current happens to be created, the dominant force in this layer would seem to be unsteady inertia and Coriolis force, implying good conditions for the maintenance of inertial oscillations.

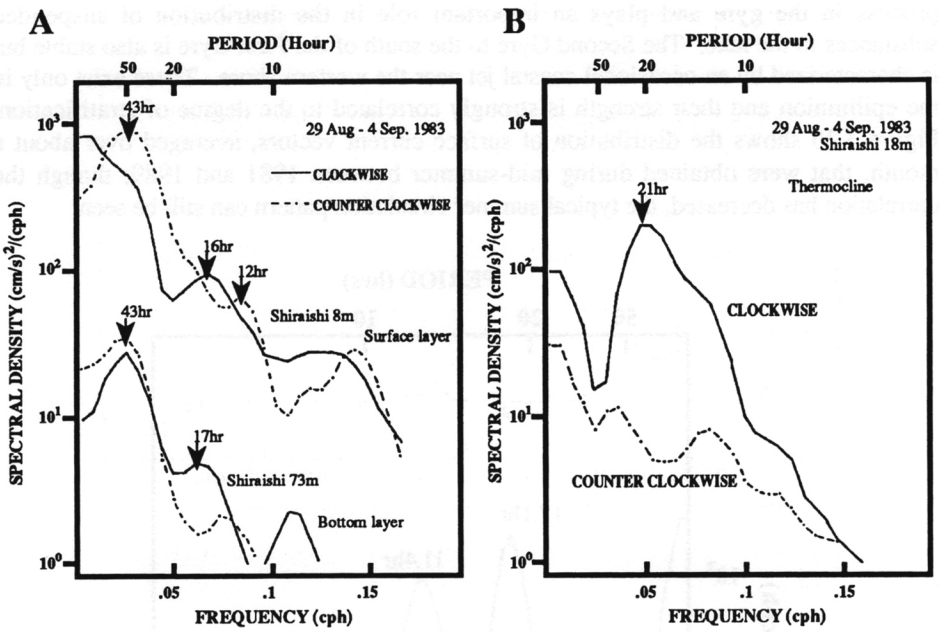

Figure 3.13. Rotary spectra of currents shown in Figure 3.12 (after Endoh and Okumura, 1989).

In the stratification period, short-period baroclinic oscillations occur frequently. The period of these oscillations depend on the intensity of stratification and were 17 hours in May and 11 hours in August (Figure 3.14). Csanady (1973) showed that the frequency σ of the internal Poincaré wave in a channel of width b may be expressed as:

$$\sigma = f\,(1 + R^2\,\pi^2/b^2)^{1/2},$$

where f is the Coriolis' parameter ($8.4 \times 10^{-5}\ s^{-1}$) and R is the internal radius of deformation. The internal radius of deformation calculated using the observed water temperatures was 2.4 km in May and 6.2 km in August. The corresponding periods of the internal Poincaré wave was therefore, 18.5 hour and 12.6 hour respectively, almost coinciding with the observed periods.

Conclusion

According to the recent current measurements in the North Basin of Lake Biwa, the cyclonic gyre (the First Gyre) is quite stable in the surface layer during the period of thermal stratification. This gyre sustains a weak large scale vertical circulation with sinking at the cool central core. This subsidiary circulation is considered to be a decay

process in the gyre and plays an important role in the distribution of suspended substances in the lake. The Second Gyre to the south of the First Gyre is also stable but is characterized by an occasional coastal jet near the western shore. These exist only in the epilimnion and their strength is strongly correlated to the degree of stratification. Figure 3.15 shows the distribution of surface current vectors, averaged over about a month, that were obtained during mid-summer between 1981 and 1989; though the correlation has decreased, the typical summer circulation pattern can still be seen.

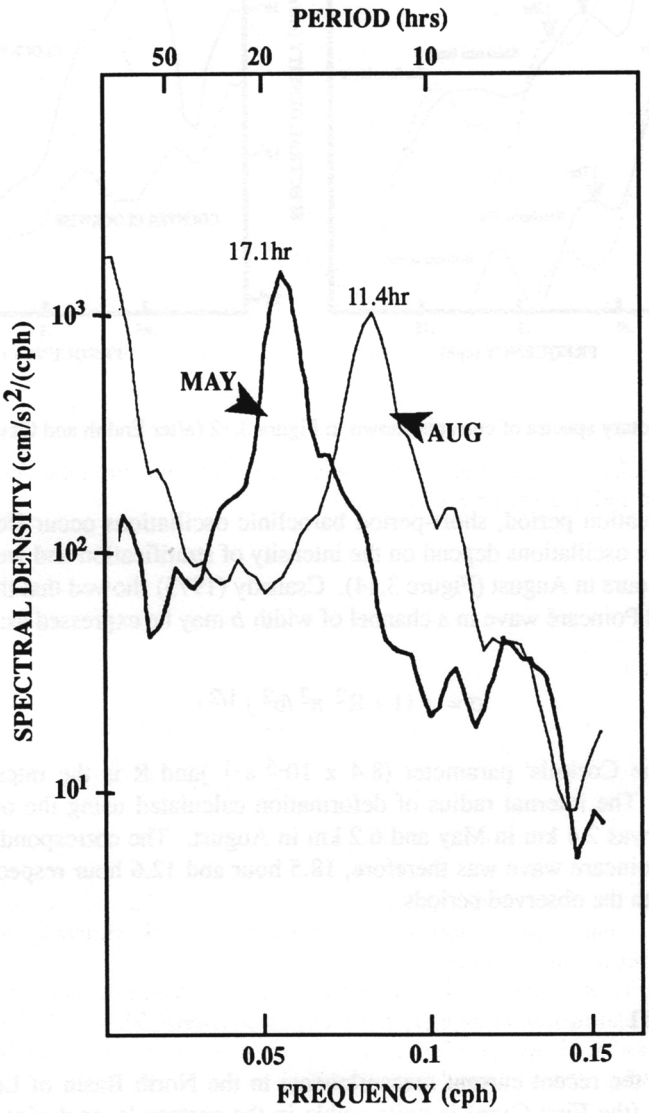

Figure 3.14. Rotary spectra (clockwise components) of the surface current in May and August. These spectral peaks correspond to the internal Poincare wave (after Endoh and Okumura, 1989).

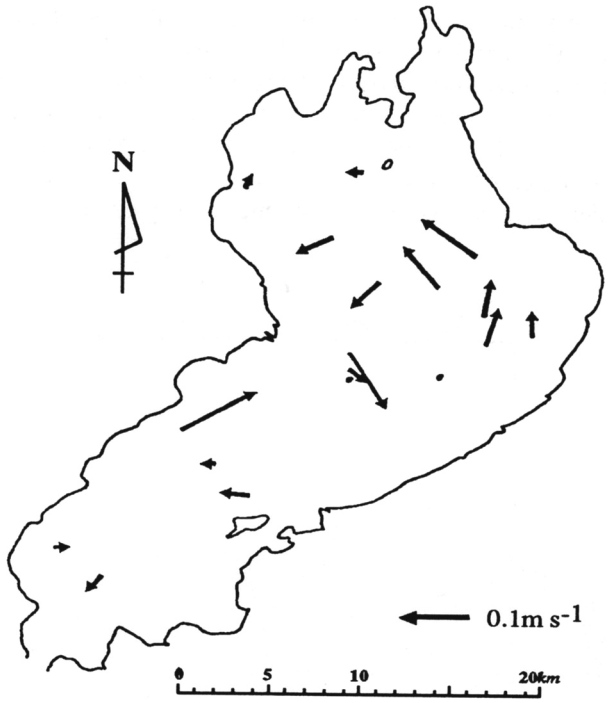

Figure 3.15. Horizontal distribution of time-averaged surface currents in the North Basin of Lake Biwa measured during the summer of 1981-1989.

References

Csanady, G. T., (1973) Transverse internal seiches in large oblong lakes and marginal seas. *J Phys. Oceanogr.*, 3: 439-447.

Endoh, S., (1978) Diagnostic analysis of water circulations in Lake Biwa. *J. Oceanogr Soc. Japan,* 34: 250-260.

Endoh, S., (1986) Diagnostic study on the vertical circulation and the maintenance mechanisms of the cyclonic gyre in Lake Biwa. *J. Geophys. Res.*, 91C1: 869-876.

Endoh, S., I. Okamoto, Y Okumura, T Tamura, K. Takano, Y Hamai, T Kodani, Y Hayami, H. Asada, H. Kawamura and K. Iwane, (1987) Measurements of lake current by using radar. *Mem. Fac. Educ., Shiga Univ* 37: 27-38.(J)

Endoh, S. and Y Okumura, (1989) Continuous current measurements in Lake Biwa (II) time variations of lake currents in the northern basin. *Jpn. J. Limnol.* 50: 341-350.(J)

Okumura, Y and S. Endoh, (1985) Continuous current measurements in Lake Biwa (I) - method and some results. *Jpn. J. Limnol*. 46: 135-142.(J)